**Supplemental data**

# Systemic combinatorial peptide selection yields a non-canonical iron-mimicry mechanism for targeting tumors in a mouse model of human glioblastoma

Fernanda I. Staquicini, Michael G. Ozawa, Catherine A. Moya, Wouter H. P. Driessen, E. Magda Barbu, Hiroyuki Nishimori, Suren Soghomonyan, Leo G. Flores 2nd, Xiaowen Liang, Vincenzo Paolillo, Mian M. Alauddin, James P. Basilion, Frank B. Furnari, Oliver Bogler, Frederick F. Lang, Kenneth D. Aldape, Gregory N. Fuller, Magnus Höök, Juri G. Gelovani, Richard L. Sidman, Webster K. Cavenee, Renata Pasqualini and Wadih Arap

**Supplemental Table 1**

Expression of RMTs in GBM compared to normal brain (NB)*

| Affymetrix ID | Gene Symbol | Gene Title | Ratio GBM/NB | *P*-value (*t*-test) |
|---|---|---|---|---|
| 208691_at | TFRC | Transferrin receptor (p90, CD71) | 2.1 | $3.83 \times 10^{-33}$ |
| 202068_s_at | LDLR | Low density lipoprotein receptor | 1.6 | $1.02 \times 10^{-05}$ |
| 207332_s_at | TFRC | Transferrin receptor (p90, CD71) | 1.4 | $1.91 \times 10^{-27}$ |
| 202067_s_at | LDLR | Low density lipoprotein receptor | 1.1 | 0.033619 |
| 209894_at | LEPR | Leptin receptor | 1.0 | 0.702604 |
| 217183_at | LDLR | Low density lipoprotein receptor | 1.0 | 0.039231 |
| 217103_at | LDLR | Low density lipoprotein receptor | 1.0 | 0.002134 |
| 217173_s_at | LDLR | Low density lipoprotein receptor | 0.9 | 0.122683 |
| 217005_at | LDLR | Low density lipoprotein receptor | 0.9 | 0.125734 |
| 207851_s_at | INSR | Insulin receptor | 0.8 | 0.003325 |
| 207255_at | LEPR | Leptin receptor | 0.8 | 0.046729 |
| 211354_s_at | LEPR | Leptin receptor | 0.7 | 0.738849 |
| 211355_x_at | LEPR | Leptin receptor | 0.7 | 0.075484 |
| 211356_x_at | LEPR | Leptin receptor | 0.6 | 0.058692 |

*Gene expression ratio of RMTs in GBM versus NB is shown from the highest (TFRC) to lowest (LEPR) level of relative gene expression.

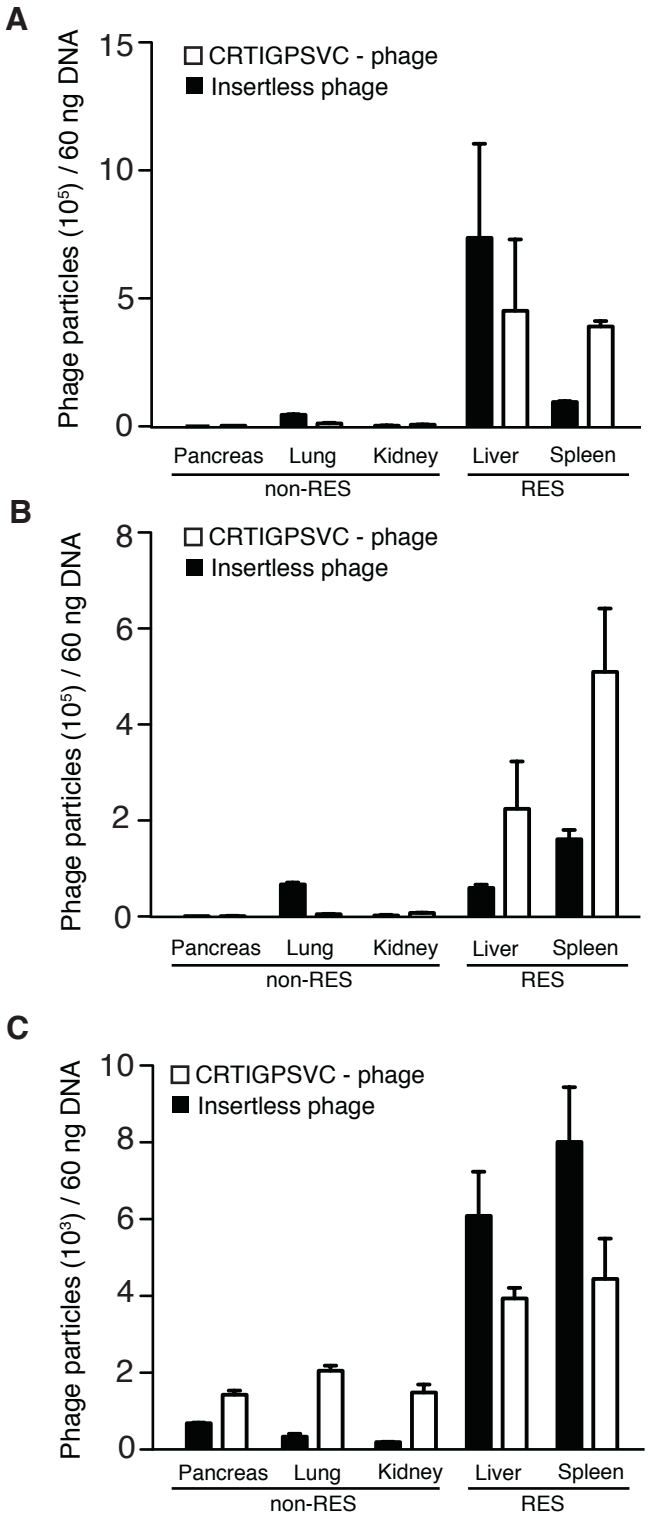


**Supplemental Figure 1**. Mice were injected with $10^{10}$ TU of phage and organs were collected after 10 min (A), 30 min (B) and 24 h (C) of systemic circulation. Accumulation of phage particles is observed in the spleen and liver under all experimental conditions, a phenomenon caused by the non-specific clearance of phage within the RES.

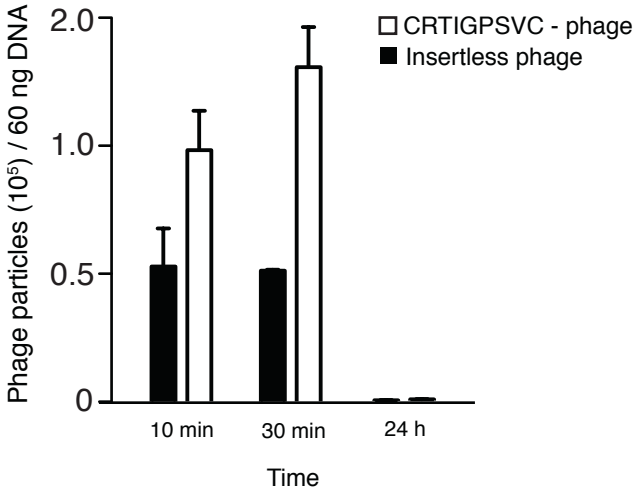


**Supplemental Figure 2.** In vivo homing of targeted and control phage to the bone marrow of normal mice. Mice were injected with $10^{10}$ TU of phage and bone marrow was collected after 10 min, 30 min and 24 h of systemic circulation.

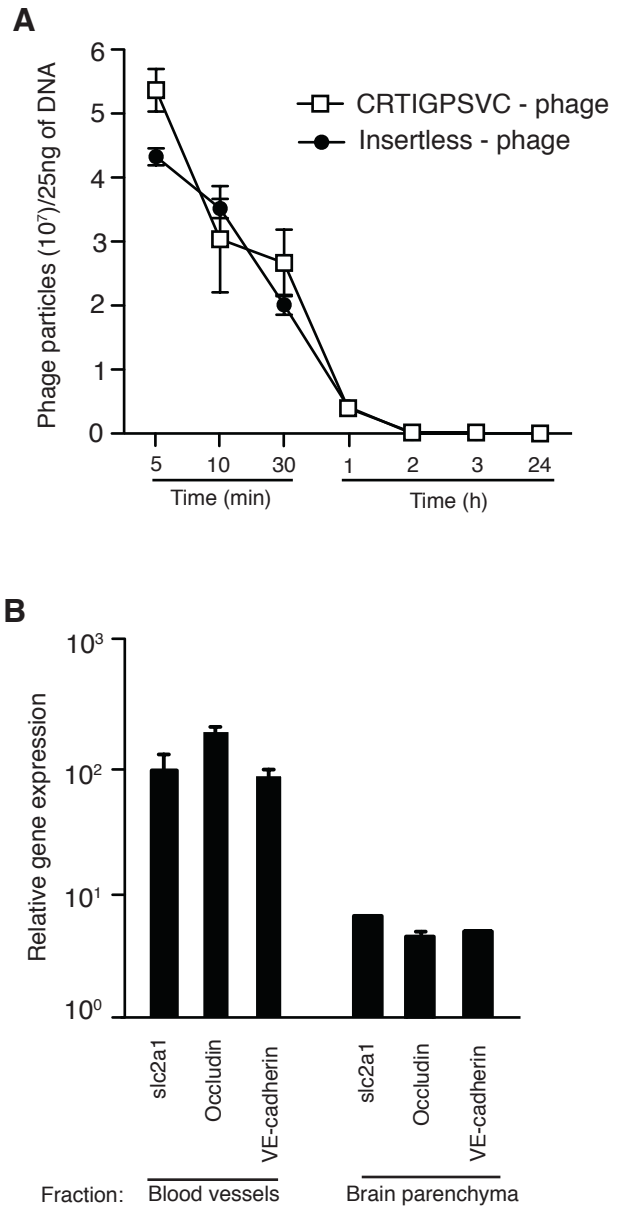


**Supplemental Figure 3.** (A) Pharmacokinetic study of targeted and insertless phage half-lives in blood. (B) Separation of microvessels from the brain parenchyma was confirmed by real-time quantitative PCR. Shown are markers of brain capillaries (slc2a1 and occludin) and large blood vessels (VE-cadherin).

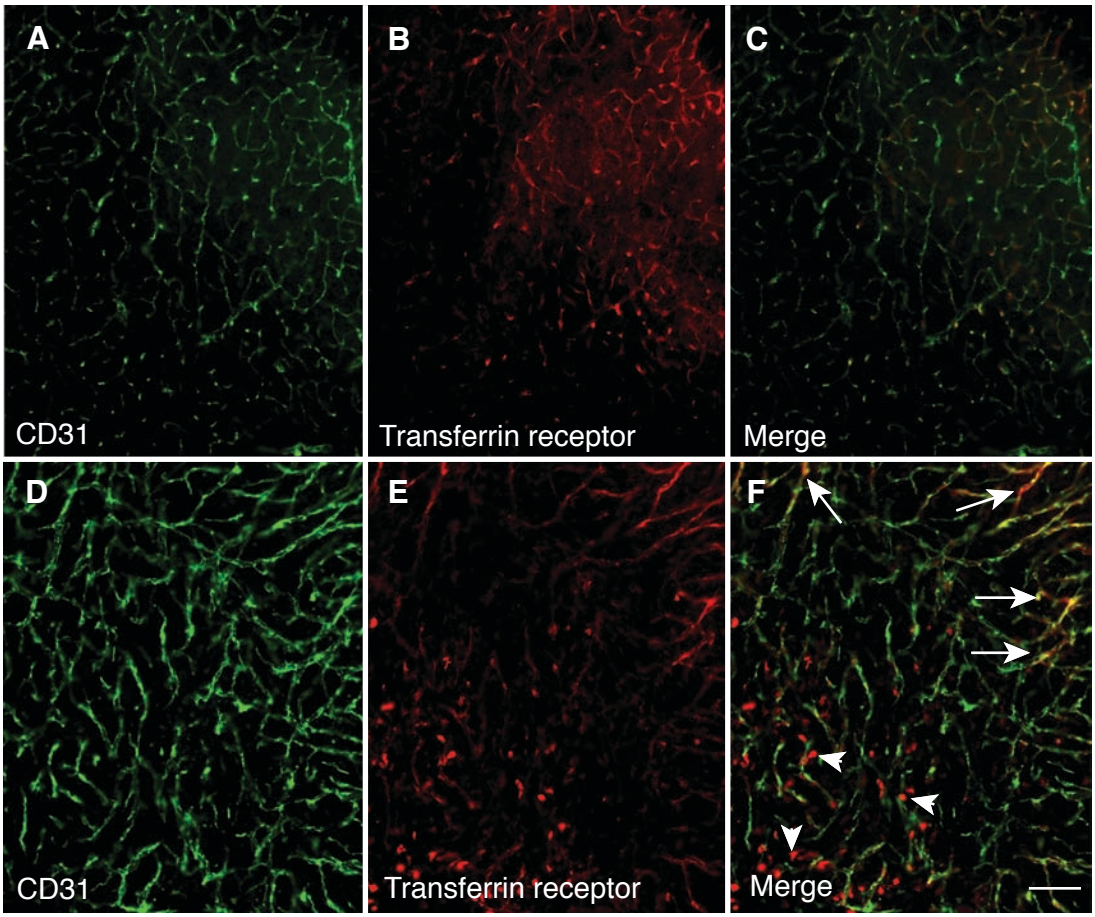


**Supplemental Figure 4.** Expression of TfR in normal brain and human glioblastoma xenograft. (A-F) CD31 (green) and TfR (red) immunofluorescence demonstrate expression of TfR in both normal (A-C) and tumor tissues (D-F). (E) High levels of expression of TfR, in parallel with the increased capillary density are observed in brain tumor. (F) Merged image show co-localization of TfR and CD31 in angiogenic blood vessels of human glioblastoma grafts. Arrows: tumor blood vessels; arrowhead: tumor stroma. Scale bar, 100 μm.

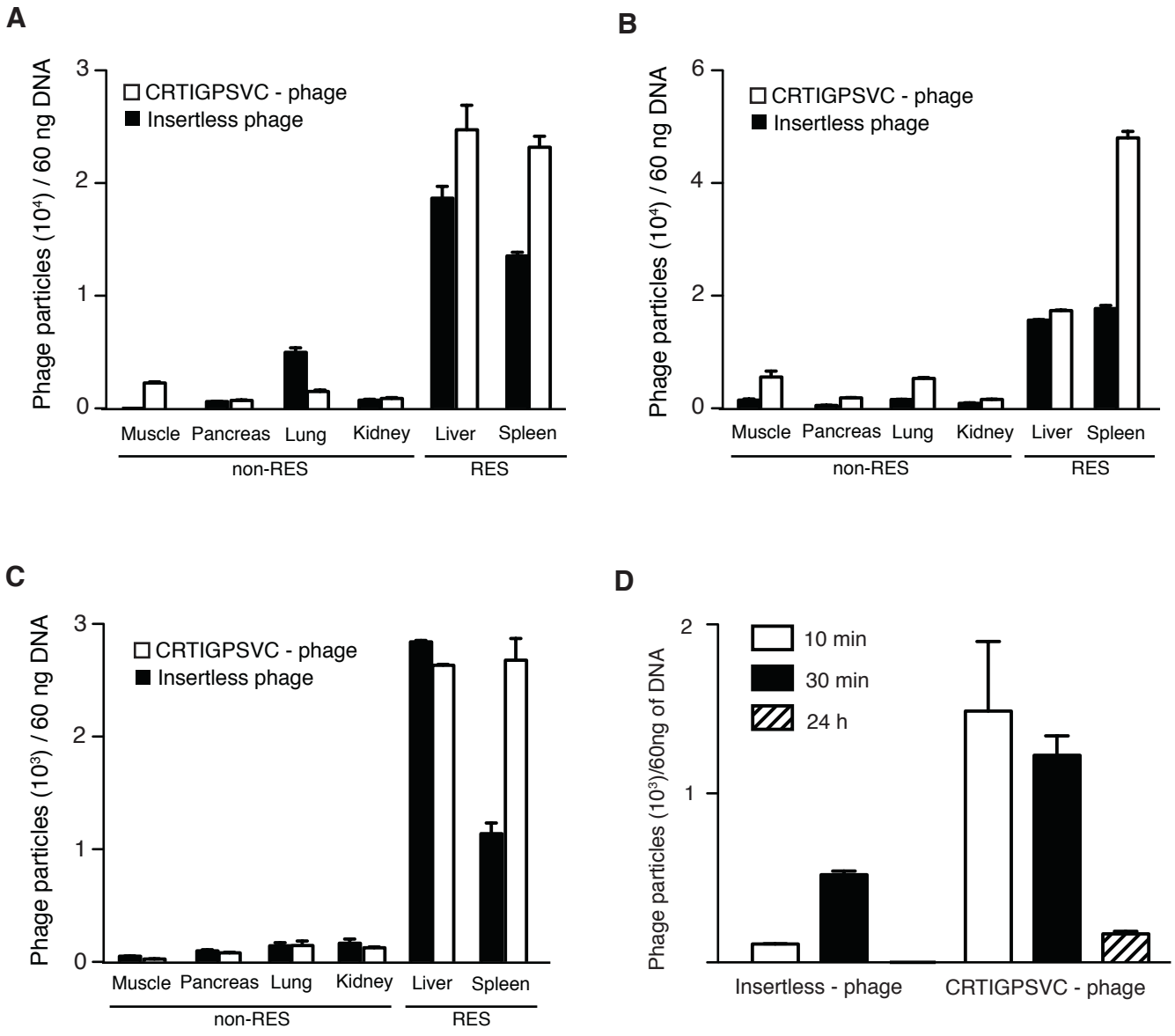


**Supplemental Figure 5.** (A-D) Mice were injected with $10^{10}$ TU of phage and organs were collected after 10 min (A), 30 min (B) and 24 h (C) of systemic circulation. (D) Homing of CRTIGPSVC-phage to subcutaneous brain tumor.

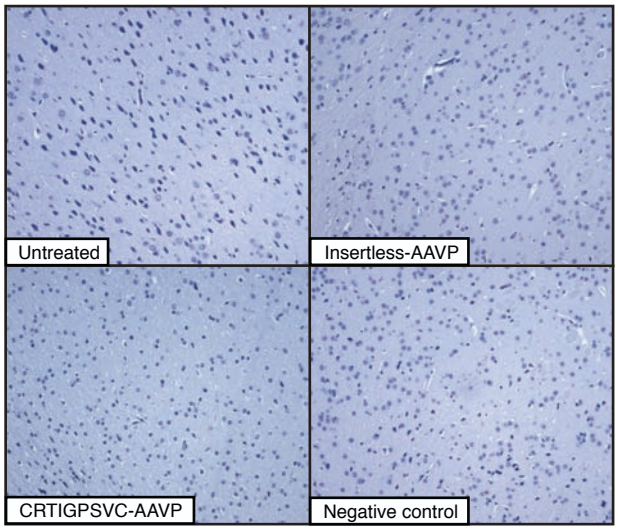


**Supplemental Figure 6.** Detection of apoptotic cells by TUNEL was performed on normal brain tissue sections of animals treated with control insertless AAVP or with targeted-AAVP. Untreated animals received only vehicle. Non-immune IgG was used as negative control.